Supplementary document

Experimental and Computational Investigation of the Influence of Stoichiometric Mixture Fraction on Structure and Extinction of Laminar, Nonpremixed Dimethyl Ether Flames

Gerald Mairinger, Rohit Sanjay Khare, Krithika Narayanaswamy, Martin Hunyadi-Gall, Vasudevan Raghavan, Kalyanasundaram Seshadri

The computational results for the extinction strain rates obtained using the San Diego mechanism show significant deviation in Fig. S1 when compared against the experimental values. To identify the reactions that impact the extinction strain rates the most, sensitivity coefficients for all reactions towards peak temperatures are obtained at all values of ξ_{st} for DME-oxidizer mixtures at strain rates close to extinction. It is observed that updating the rate constants of the reactions to which peak temperatures are most sensitive to, based on more recent and reliable sources, results in little differences in strain rates at all ξ_{st}. Therefore, individual pathways in the San Diego mechanism are manually inspected to identify the reactions important for predicting extinction strain rates at high ξ_{st} conditions. This kinetic analysis is discussed in the following.

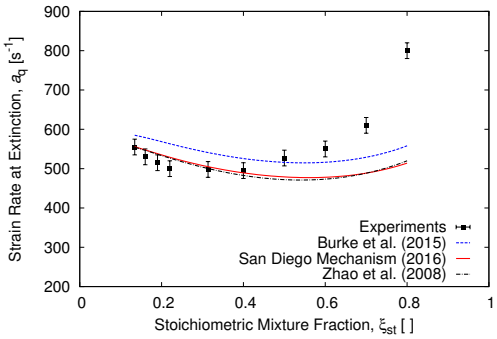

Figure S1: Extinction strain rate plotted as a function of stoichiometric mixture fraction (ξ_{st}) for DME laminar non-premixed flame.

1 Kinetic analysis for prediction of extinction strain rates at varied stoichiometric mixture fractions

Mixtures with high values of ξ_{st} are characterized by high concentration of oxygen (and low concentration of nitrogen) on the oxidizer side. Thus, large amounts of O and OH radicals are expected to be present at these conditions. After a careful examination of the reactions involving O atoms and OH radicals, it is concluded that the reactions of OH radicals are the most important in predicting the extinction strain rates at high ξ_{st}. This is also in corroboration with a recent study [1] reporting extinction strain rates of large hydrocarbon fuels. A set of reactions involving OH radicals is thus identified, and the rate constants of involved reactions have been updated based on more recent estimations or calculations from literature. Table 1 lists these reactions along with new rate parameters assigned to them and the sources from where they have been obtained. It should be noted that the revised rate constants are all based on existing studies, and not tuned to replicate any experimental data set.

Reaction	A	n	E_a
(1) $CH_2O + O \leftrightharpoons HCO + OH$			
(a) San Diego Mechanism [2]	3.50E+13	0.00	14.7
(b) Updated Mechanism [3]	3.29E+07	1.94	4.34
(2) $CH_3 + HO_2 \leftrightharpoons CH_3O + OH$			
(a) San Diego Mechanism [4]	5.00E+12	0.00	0.00
(b) Updated Mechanism [5]	1.81E+13	0.00	0.00
(3) $CH_3O + OH \leftrightharpoons CH_2O + H_2O$			
(a) San Diego Mechanism [6]	5.00E+12	0.00	0.00
(b) Updated Mechanism [7]	3.55E+02	2.50	7.89
(4) $CH_3OCH_3 + O \leftrightharpoons CH_3OCH_2 + OH$			
(a) San Diego Mechanism	$--$	$--$	$--$
(b) Updated Mechanism [8]	2.69E+07	2.00	11.00

Table 1: Rate parameters in the Arrhenius form $k = AT^n \exp(-E_a/R_uT)$. Units are mol, s, cm^3, kJ, and K. Reaction (4) is added to the San Diego mechanism.

Results and discussion:

Figure S2 depicts the comparison between experiments and the simulations performed using the updated mechanism with the revised rate parameters for the reactions listed in Table 1. It is important to note that, the increase in the extinction strain rates at higher ξ_{st} is a combined effect of revisions made in all the reaction rate constants indicated in Table 1, and is found not to be dominated by any one of those modifications. These results are in reasonable agreement with the experimental results except at the largest ξ_{st} value. The updated mechanism is able to predict the extinction strain rate at low ξ_{st} within the experimental uncertainty, where the results from San Diego mechanism are closer to experimental values. Further, the updated model is also able to predict the local minimum attained by the extinction strain rate in accordance with the experiments, which is not the case with the San Diego mechanism. Furthermore, it is able to predict the increase in strain rate at a faster rate at higher ξ_{st}, similar to the experimental data for $\xi_{st} \leq 0.7$, where San Diego mechanism shows notable deviations.

Comparing the amounts of OH radical within the flame predicted using the original San Diego mechanism [9] and the updated model, the important role played by this radical in increasing the strain rates at extinction at higher ξ_{st} can be realised. Figure S3 shows that OH is present in higher amounts at larger ξ_{st} (0.7) when using the updated model compared to the San Diego mechanism, while displaying hardly any differences at smaller ξ_{st} (0.19) between the two models.

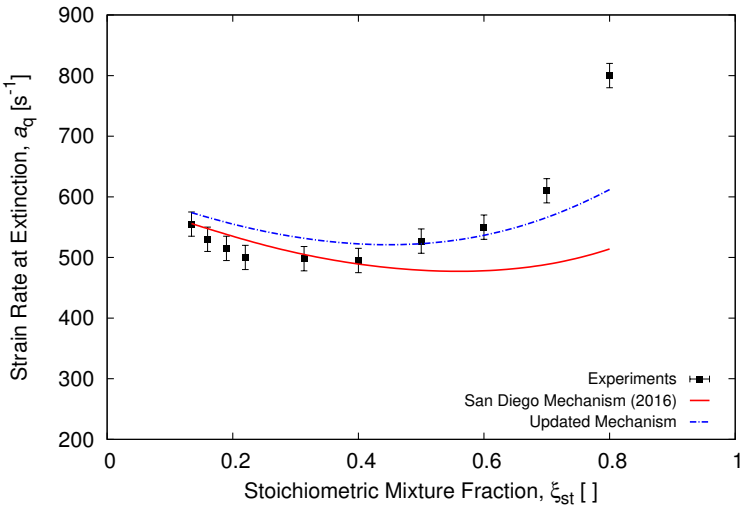

Figure S2: Improved agreement with experimental values with the updated mechanism at high ξ_{st}.

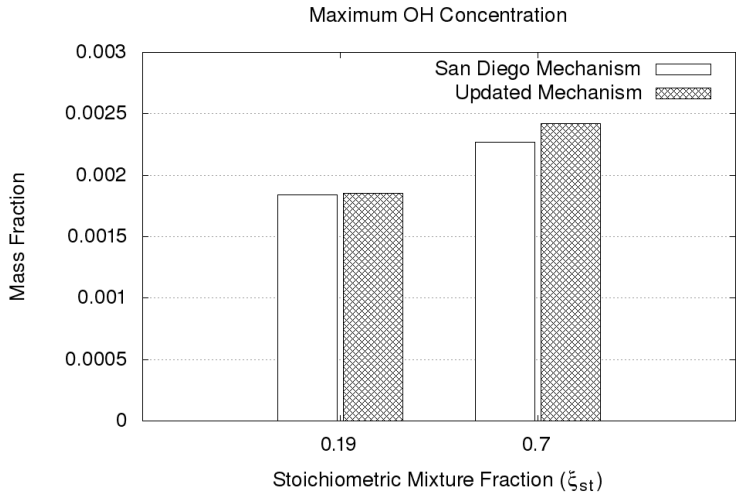

Figure S3: Maximum OH concentration at $\xi_{st} = 0.19$ and $\xi_{st} = 0.7$.

2 Validation results for DME with the updated mechanism

A consistency check is performed to identify the performance of the updated mechanism towards predicting the results for DME oxidation in other configurations that the original San Diego mechanism has been validated against. These results are shown in Figs. S4–S6 for ignition delays [10], flame speeds [11, 12] of DME as well as species profiles in a flow reactor [13], respectively.

Considering the results for ignition delays (Fig. S4) and flow reactors (Fig. S6) for DME, it is seen that the updated mechanism performs as well as the San Diego mechanism [9]. With respect to flame speeds (Fig. S5), for lean mixtures ($\phi < 1$), the updated mechanism deviates from the experimental values, even though this may be reasonable considering the scatter in the experimental data sets.

- Ignition Delays:

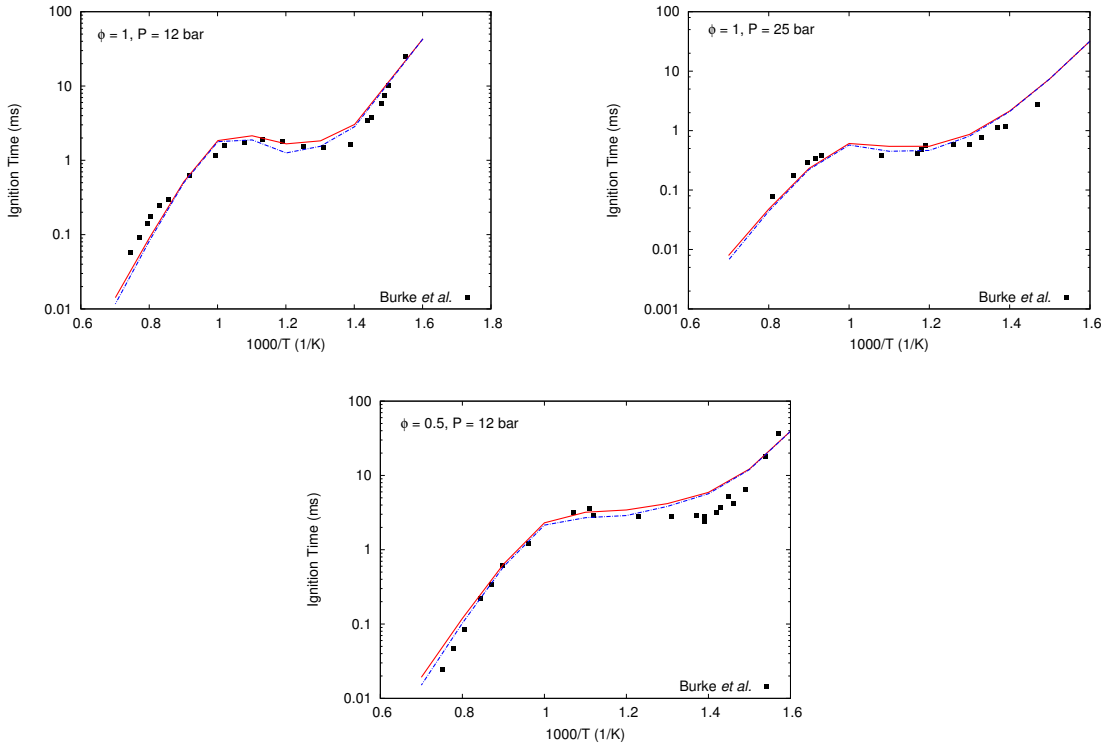

Figure S4: Ignition delay times for DME-air mixtures for a range of equivalence ratios (ϕ) and pressures. Symbols – experimental data from Burke *et al.* [10]; lines – simulations: San Diego mechanism (red solid lines), updated mechanism (blue dashed lines)

- Flame Speeds:

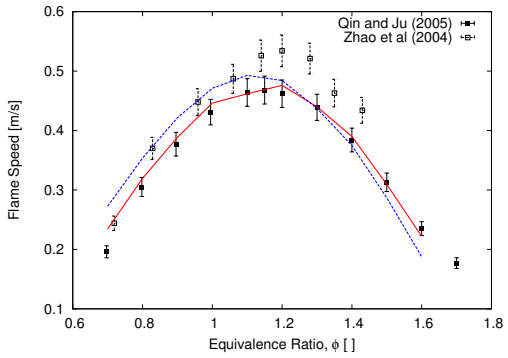

Figure S5: Laminar burning velocities of DME-air mixtures at T_u = 300 K and p = 1 atm. Symbols – experiments: Qin and Ju [11] (filled symbols), Zhao *et al.* [12] (hollow symbols); lines – simulations: San Diego mechanism (red solid lines), updated mechanism (blue dashed lines).

- Species Profiles:

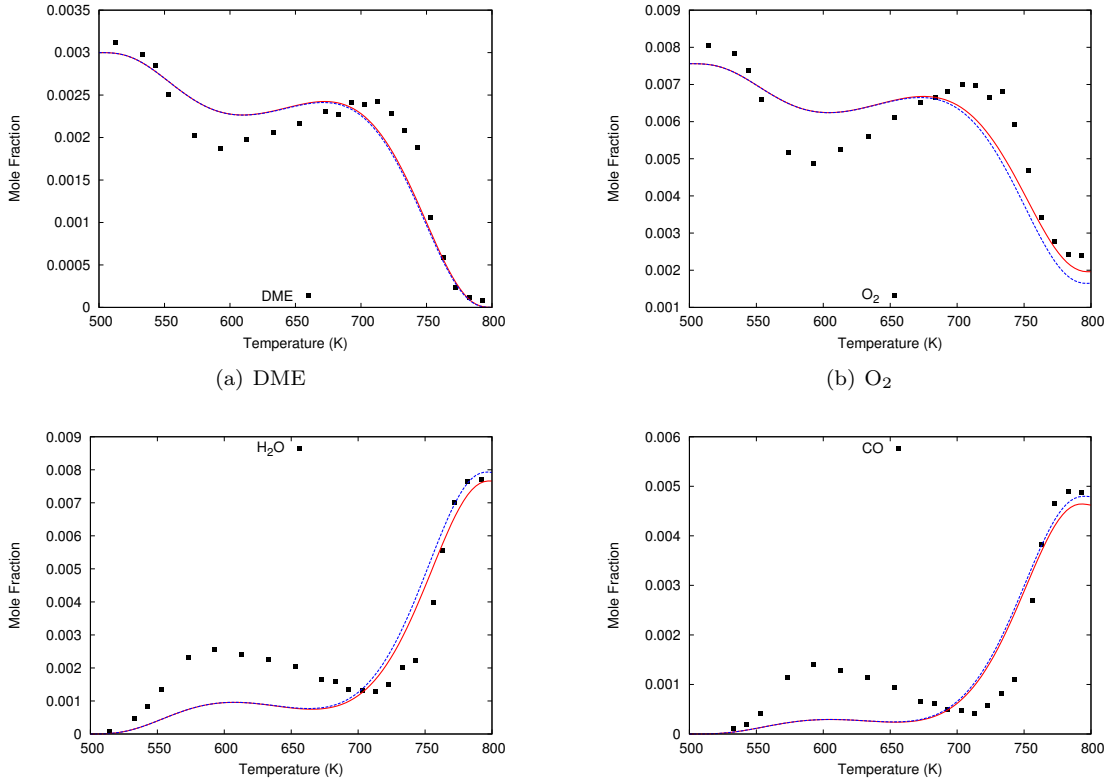

(a) DME (b) O_2

(c) H_2O (d) CO

Figure S6: Species profiles in a constant pressure flow reactor, $\phi = 1.19$, 0.3% DME in N_2 at 12.5 atm. Symbols – experimental data from Fischer *et al.* [13]; lines – simulations: San Diego mechanism (red solid lines), updated mechanism (blue dashed lines).

3 Validation results for methanol and methane

Since the San Diego mechanism is valid for methane as well as methanol apart from DME, predictions from the updated mechanism are also assessed for these two fuels. These results, which reassure that the updated model performs as good as the original San Diego mechanism [9], are shown in Figs. S7–S11.

3.1 Results for methanol

For methanol, the results from the updated mechanism are compared with results from the San Diego mechanism as well as a 38 step mechanism derived for methanol by Tarrazo *et al.* [14]. Here, exhaustive validation tests for methanol is not shown, and only some representative cases are shown.

- Ignition Delays:

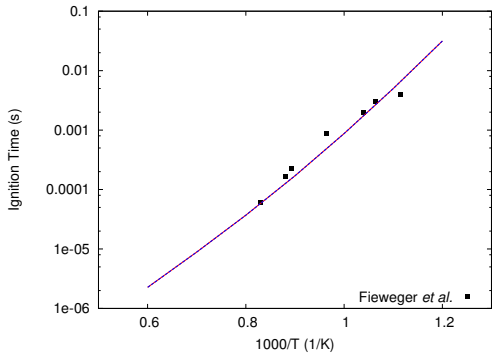

Figure S7: Ignition delay times for methanol-air mixtures at $\phi = 1$, p = 13 atm. Symbols – experimental data from Fieweger *et al.* [15]; lines – simulations: San Diego mechanism (red solid lines), updated mechanism (blue dashed lines), 38-step mechanism (dot-crossed magenta lines).

- Flame Speeds:

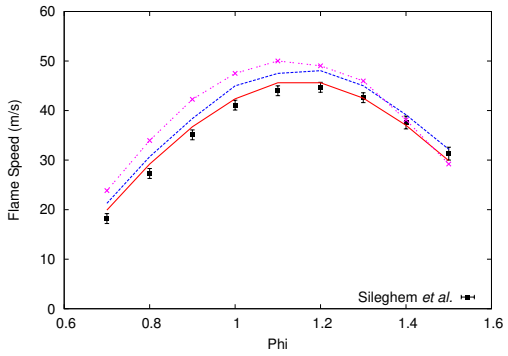

Figure S8: Laminar burning velocities of methanol-air mixtures at T_u = 300 K and p = 1 atm. Symbols – experimental data from Sileghem *et al.* [16]; lines – simulations: San Diego mechanism (red solid lines), updated mechanism (blue dashed lines), 38-step mechanism (dot-crossed magenta lines).

- Extinction Strain Rates:

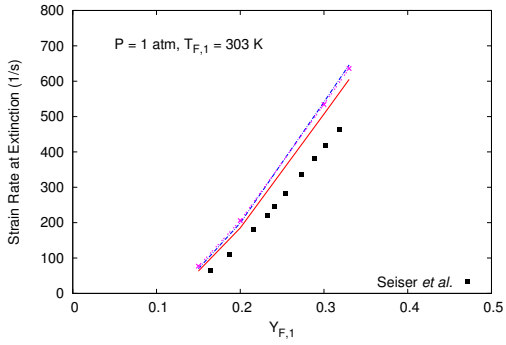

Figure S9: Strain rate at extinction plotted as a function of the mass fraction of fuel in the fuel stream. Symbols – experimental data from Seiser *et al.* [17]; lines – simulations: San Diego mechanism (red solid lines), updated mechanism (blue dashed lines), 38-step mechanism (dot-crossed magenta lines).

3.2 Results for methane

- Ignition Delays:

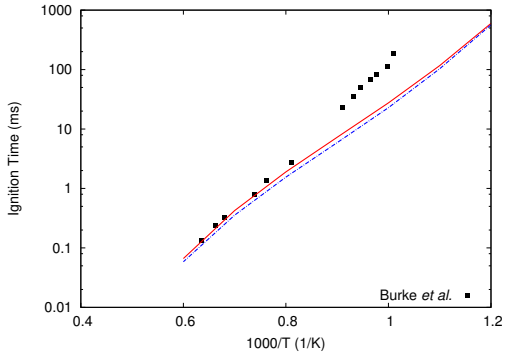

(a) CH_4

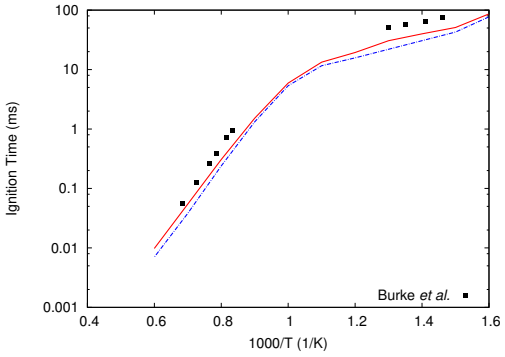

(b) 80/20 CH_4/DME

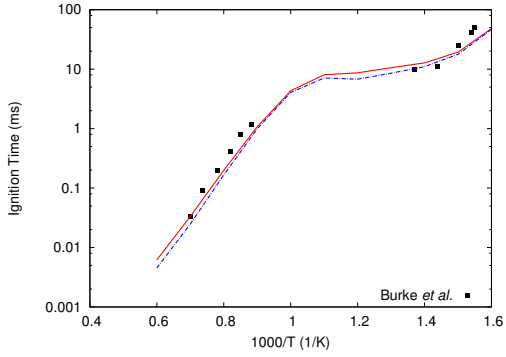

(c) 60/40 CH_4/DME

Figure S10: Ignition delay times at p = 7−10 atm for pure CH_4 and binary blends of 80/20 CH_4/DME and 60/40 CH_4/DME. Symbols – experimental data from Burke *et al.* [10]; lines – simulations: San Diego mechanism (red solid lines), updated mechanism (blue dashed lines).

- Flame Speeds:

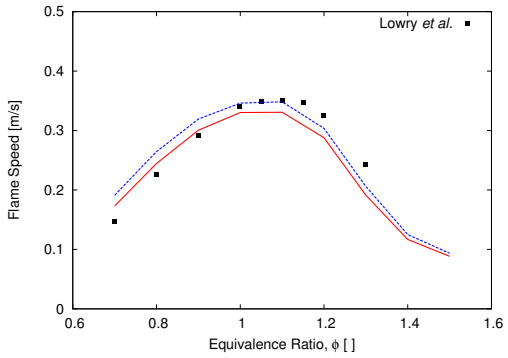

Figure S11: Laminar burning velocities of methane-air mixtures at T_u = 300 K and p = 1 atm. Symbols – experimental data from Lowry *et al.* [18]; lines – simulations: San Diego mechanism (red solid lines), updated mechanism (blue dashed lines).

4 Summary and Remarks

In summary, to understand the differences between predictions and measurements of strain rates at extinction shown by the San Diego mechanism from the chemical kinetic model point of view, a detailed analysis is undertaken. Starting with the San Diego mechanism, revisions to the rate constants of important reactions producing and consuming OH radicals, which are key to describing the extinction behaviour have been suggested. These revisions are based on more recent estimations or rate constant calculations reported in literature.

The updated model is able to reproduce the extinction strain rates of DME at low through high ξ_{st}, for $\xi_{st} \leq 0.7$. The higher resistance to extinction predicted by the model at higher ξ_{st} is found to be due to the increased OH concentration at those conditions compared to those at lower ξ_{st}. Further, the updated mechanism has been comprehensively assessed and found to satisfactorily predict the combustion characteristics such as ignition delays, species profiles, and laminar flame speeds of DME, as well as those of methanol and methane, which the original San Diego mechanism is valid for, indicating that the revisions suggested are valid and consistent.

Nonetheless, the updated model is unable to explain the rapid rise of extinction strain rate of DME measured at high ξ_{st} (particularly at $\xi_{st} = 0.8$). Despite the consistency in the updated model demonstrated by the presented validation results for DME, methane, as well as methanol, the inability of the revised reaction mechanism to predict the extinction behavior at very high ξ_{st} points to possible missing pathways in the DME mechanism, as indicated in the main article.

References

[1] S.H. Won, S. Dooley, F.L. Dryer, Y. Ju, A radical index for the determination of the chemical kinetic contribution to diffusion flame extinction of large hydrocarbon fuels, Combust. Flame 159 (2012) 541–551.

[2] J. Warnatz, Rate coefficients in the C/H/O system. Combust. Chem. (1984) 197–360.

[3] J.T. Herron, Evaluated chemical kinetic data for the reactions of atomic oxygen o (3p) with saturated organic compounds in the gas phase, J. Phys. Chem. Ref. Data 17 (1988) 967–1026.

[4] M. Frenklach, H. Wang, M.J. Rabinowitz, Optimization and analysis of large chemical kinetic mechanisms using the solution mapping methodcombustion of methane, Prog. Energy Combust. Sci. 18 (1992) 47–73.

[5] D.L. Baulch, C. Cobos, R.A. Cox, C. Esser, P. Frank, T. Just, J.A. Kerr, M.J. Pilling, J. Troe, R.W. Walker, Evaluated kinetic data for combustion modelling, J. Phys. Chem. Ref. Data 21 (1992) 411–734.

[6] S.C. Li, F.A. Williams Formation of NOx, CH4, and C2 species in laminar methanol flames, Symp. (Int.) Combust. 27 (1998) 485–493.

[7] A.W. Jasper, S.J. Klippenstein, L.B. Harding, Theoretical rate coefficients for the reaction of methyl radical with hydroperoxyl radical and for methylhydroperoxide decomposition, Proc. Combust. Inst. 32 (2009) 279–286.

[8] K. Takahashi, O. Yamamoto, T. Inomata, M. Kogoma, Shock-tube studies on the reactions of dimethyl ether with oxygen and hydrogen atoms, Int. J. Chem. Kinet. 39 (2007) 97–108.

[9] The San Diego Mechanism, Version 2016-08-15, `http://web.eng.ucsd.edu/mae/groups/combustion/mechanism.html`.

[10] U. Burke, K.P. Somers, P. OToole, C.M. Zinner, N. Marquet, G. Bourque, E.L. Petersen, W.K. Metcalfe, Z. Serinyel, H.J. Curran, An ignition delay and kinetic modeling study of methane, dimethyl ether, and their mixtures at high pressures, Combust. Flame 162 (2015) 315–330.

[11] X. Qin, Y. Ju, Measurements of burning velocities of dimethyl ether and air premixed flames at elevated pressures, Proc. Combust. Inst. 30 (2005) 233–240.

[12] Z. Zhao, A. Kazakov, F.L. Dryer, Measurements of dimethyl ether/air mixture burning velocities by using particle image velocimetry, Combust. Flame 139 (2004) 52–60.

[13] S.L. Fischer, F.L. Dryer, H.J. Curran, The reaction kinetics of dimethyl ether. i: high-temperature pyrolysis and oxidation in flow reactors, Int. J. Chem. Kinet. 32 (2000) 713–740.

[14] E. Fernández-Tarrazo, M. Sánchez-Sanz, A.L. Sánchez, F.A. Williams, A multipurpose reduced chemical-kinetic mechanism for methanol combustion, Combust. Theor. Model. 20 (2016) 613–631.

[15] K. Fieweger, R. Blumenthal, G. Adomeit, Self-ignition of SI engine model fuels: a shock tube investigation at high pressure, Combust. Flame 109 (1997) 599–619.

[16] L. Sileghem, V.A. Alekseev, J. Vancoillie, E.J.K. Nilsson, S. Verhelst, A.A. Konnov, Laminar burning velocities of primary reference fuels and simple alcohols, Fuel 115 (2014) 32–40.

[17] R. Seiser, S. Humer, K. Seshadri, E. Pucher, Experimental investigation of methanol and ethanol flames in nonuniform flows, Proc. Combust. Inst. 31 (2007) 1173–1180.

[18] W. Lowry, J. Vries, M. Krejci, E. Petersen, Z. Serinyel, W. Metcalfe, H. Curran, G. Bourque, Laminar flame speed measurements and modeling of pure alkanes and alkane blends at elevated pressures, J. Eng. Gas Turb. Power 133 (2011) 9–15.